Chemical and Process Engineering 2012, 33 (2), 263-277
DOI: 10.2478/v10176-012-0026-x

RATE OF CORROSION OF WATERWALLS IN SUPERCRITICAL PULVERISED FUEL BOILERS

Marek Pronobis, Rafał Litka*

Silesian University of Technology in Gliwice, Institute of Power Engineering and Turbomachinery, ul. Konarskiego 20, 44-100 Gliwice, Poland

This paper presents an analysis of the corrosion hazard in the burner belt area of waterwalls in pulverised fuel (PF) boilers that results from low-NOx combustion. Temperature distributions along the waterwall tubes in subcritical (denoted as SUB) and supercritical (SUP) boilers were calculated and compared. Two hypothetical distributions of CO concentrations were assumed in the near-wall layer of the flue gas in the boiler furnace, and the kinetics of the waterwall corrosion were analysed as a function of the local temperature of the tubes. The predicted rate of corrosion of the boiler furnace waterwalls in the supercritical boilers was compared with that of in the subcritical boilers.

Keywords: subcritical and supercritical boilers, corrosion, waterwalls

1. INTRODUCTION

Today, high-temperature corrosion is one of the greatest hazards that affects the durability of waterwalls in furnaces of power boilers. This phenomenon is strictly connected with conditions of combustion and occurs only in areas that contact flue gas with a reduced composition (zero or very little O_2 content), and thus, the phenomenon's commonly used names are "low-oxygen" corrosion or "low-NOx" corrosion, where low-oxygen conditions typically accompany combustion which uses the so-called primary methods of NO_x reduction (Harb and Smith 1990; Bukowski et al. 2009). Before the introduction of low NOx combustion methods, the lifetime of waterwalls exceeded 10 or more years, while now even in subcritical boilers (denoted as SUB) it does not exceed 5 - 6 years. The promoters of this corrosion type are sulphur and chlorine. In Polish conditions (Karcz et al., 2005), boilers are generally fired with low-chlorine coal and sulphate, and sulphide corrosion predominates.

An attempt to estimate the kinetics of low-NOx corrosion has been presented by Pronobis et al. (2010), where the method was also used to determine the map of the rate of the thickness loss in the waterwall tubes. In subcritical boilers, temperature's influence on the corrosion of evaporator tube, where the water-steam mixture is at a constant and relatively low temperature, is not particularly significant. However, temperature influence on the corrosion of waterwalls in supercritical (SUP) conditions is of fundamental significance. Below, the model of the process shown by Pronobis et al. (2010) was used to assess relative hazard concerning the waterwalls that operate in supercritical conditions.

*Corresponding author, e-mail: rafal.litka@polsl.pl

2. A COMPARISON OF THE OPERATING CONDITIONS OF WATERWALL TUBES IN SUB- AND SUPERCRITICAL BOILERS

On the basis of the models introduced by Pronobis et al. (2010), Nowak and Pronobis (2010) and Rusin and Wojaczek (2009), comparative calculations of temperature distribution of external surfaces in waterwall tubes in sub- and supercritical boilers were made. A hypothetical system of the boiler furnace was assumed, as shown in Fig. 1, and the graphs of the heat flux at the vertical (along the furnace height, h_f) and the horizontal coordinate axes (X_{qA_vert} and X_{qA_hor}) were assumed according to Orłowski et al. (1979) and the variant numeric calculations. It was assumed that both boilers had a tangential furnace that allowed to make the assumption that below the height of the platen superheaters, all the waterwalls are heated equally.

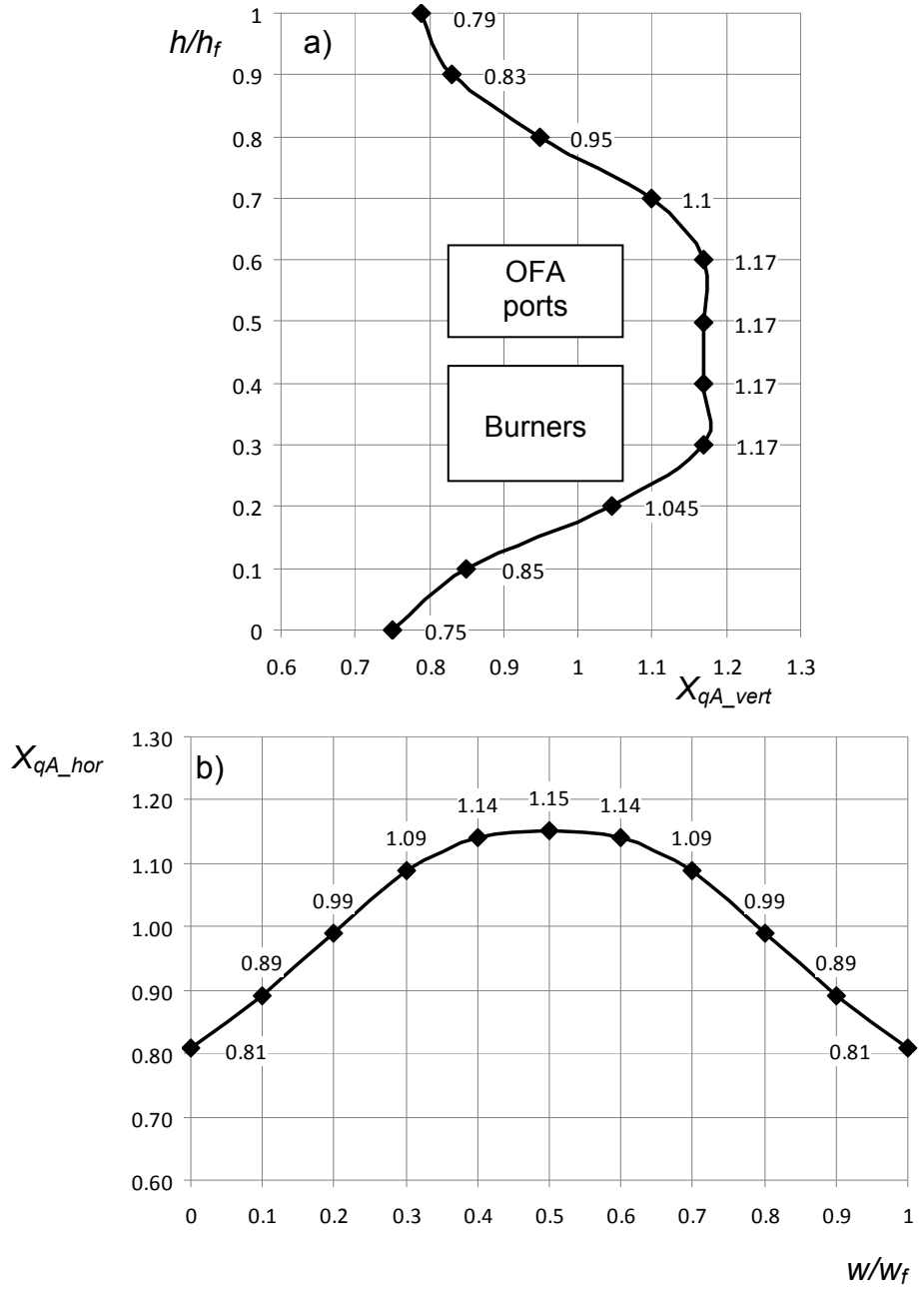

Fig. 1. Distributions of the transferred heat in the boiler furnace:
a) at the vertical coordinate axis; b) at the horizontal coordinate axis

For the subcritical unit, the assumed parameters are shown in Table 1.

Table 1. Parameters of a subcritical evaporator

Parameter	Unit	Value
Saturation pressure in separator	MPa	20.3
Saturation temperature in separator	^{o}C	367
External diameter of tubes	mm	30
Internal diameter of tubes.	mm	20
Mean flux of transferred heat.	kW/m^2	159.3
Material	-	16M

On the basis of the graphs of the heat flux distribution on the vertical and horizontal coordinate axes, a summary of the distribution of the heat transferred in the central tube of the front wall, which transferred the most heat, is shown in Fig. 2.

To better compare the results, it was assumed that the medium and local heat loads were the same in the compared boilers (volumetric q_V [kW/m^3], cross-sectional q_A [kW/m^2]), which results in identical heat fluxes reaching the waterwalls. Because of the lack of a detailed design of a supercritical boiler, the values for the calculations were assumed based on the existing subcritical boiler BP 1150 type.

The calculations of the supercritical boiler were made for two standard solutions: a boiler with waterwalls with vertical tubes with an internal ribbing (rifled tubes) and a boiler with spiral-wound waterwalls, which become vertical tubes at a level of $h/h_k = 0.6$.

The heat transfer coefficient between the subcritical steam and the water mix (nucleate boiling) was calculated with the Formula (Rassohin et al., 1970), which is valid within the scope of pressures between 8 and 20 MPa:

$$\alpha = 0.027 p^{1.33} q_A^{0.67} \tag{1}$$

where p in bar, q_A in W/m^2.

The heat transfer coefficient of water in the supercritical state was calculated using the relationship (Grabezhnaja and Kirillow, 2006):

$$Nu = 0.0052\, Re_{wm}^{0.9}\, Pr_{wm}^{0.66} \left(\frac{\bar{c}_p}{c_{p\,wm}} \right)^{0.66} \left(\frac{\rho_{m,in}}{\rho_{wm}} \right)^{0.43} \left(1 + 2.4 d/L\right) \tag{2}$$

where

$$Nu = \frac{\alpha d}{\lambda_{wm}}; \qquad Re_{wm} = \frac{(\rho w)_{wm}\, d}{\mu_{wm}} \tag{3}$$

The mean specific heat of the water is defined as

$$\bar{c}_p = \frac{h_{m,in} - h_{wm}}{t_{m,in} - t_{wm}} \tag{4}$$

and its other required properties were determined according to Wagner et al. (2000).

For relative heights between 0 and 0.2 in the subcritical boiler, an under-heating of the water to saturation temperature was assumed knowing that water flows to the waterwalls with a temperature equal to the saturation temperature in the separator, and the pressure is higher by 0.6 MPa.

2.1. Boiler with waterwall with vertical rifled tubes

The conditions that were assumed for the calculations are given in Table 2. A distribution of the heat flux was used for the middle tube of the waterwall according to Fig. 2, which was determined on the basis of the graphs shown in Fig. 1.

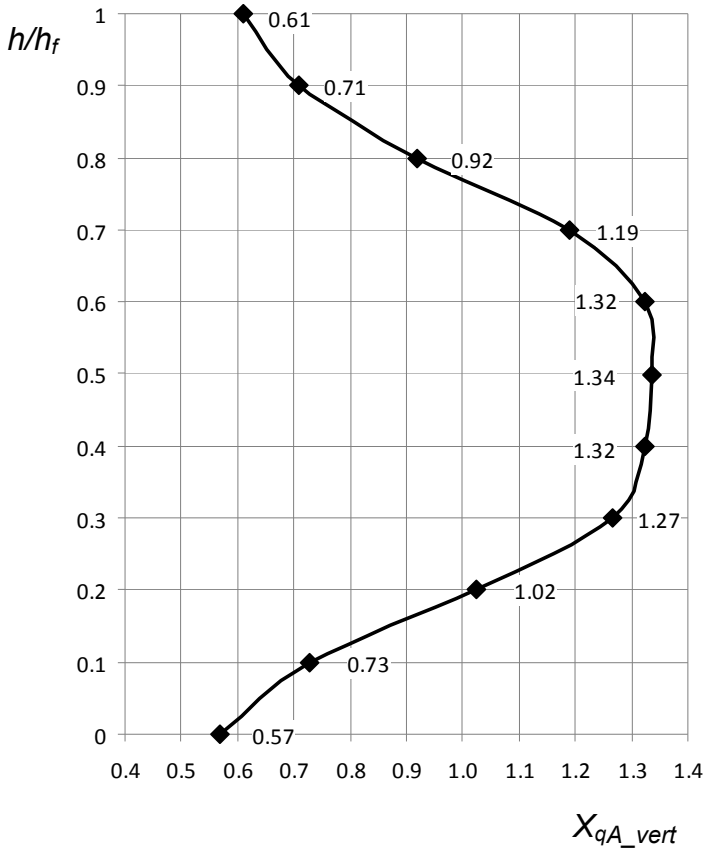

Fig. 2. Transferred heat flux distribution along the vertical coordinate axis for the middle tube of the waterwall

Because of the requirements imposed by the system of the vertical tubes in a large supercritical boiler, tubes with internal ribbing were used, as shown in Fig. 3. Such a solution corresponds to the value of the mass flux assumed in Table 2.

Table 2. Parameters of the supercritical evaporator with a waterwall of vertical tubes

Parameter	Unit	Value
Pressure at inflow	MPa	32.0
Temperature at inflow	°C	340
Pressure at outflow	MPa	31.1
Temperature at outflow	°C	473
Mass flux	kg/m^{2}s	1000
External diameter of tubes (Palkes et al., 1994)	mm	28.65
Internal diameter of tubes (mean)	mm	16.65
Height of internal ribs	mm	0.9
Mean flux of transferred heat	kW/m^2	159.3
Material	-	HCM2S

Two types of calculations were made: for tubes without an oxide scale on the inner surface and for tubes that have been in operation for a long time, which has resulted in the presence of an oxide layer. It was also assumed that in the subcritical evaporator, the thickness of the oxide layer was $\delta_{ox} = 200$ μm, and its heat conductivity was $\delta_{ox} = 1.8$ W/mK, which are typical values. For the supercritical boiler, the thickness of the oxides was calculated according to Montgomery and Karlsson (1995), as shown in Fig. 4, which was drawn by assuming a parabolic reaction rate for the oxide scale thickness for 100 000 h. For the waterwall temperatures less than 450°C, a constant thickness of $\delta_{ox} = 20$ μm was assumed. For comparative purposes, Fig. 4 also shows results when corrosion follows a linear law (Wright and Pint, 2002).

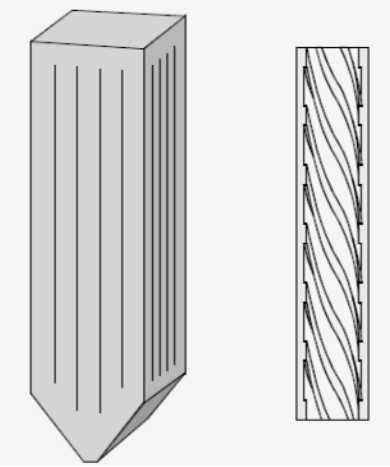

Fig. 3. Waterwall of vertical tubes with internal ribbing (Franke and Kral, 2003)

Because of the lack of data for alloy HCM2S, the kinetics of 10CrMo9-10 oxidation were used.

A list of results of the calculations for the tubes without an internal oxide layer is shown in Fig. 5, and for the tubes with an oxide scale, the results are shown in Fig. 6.

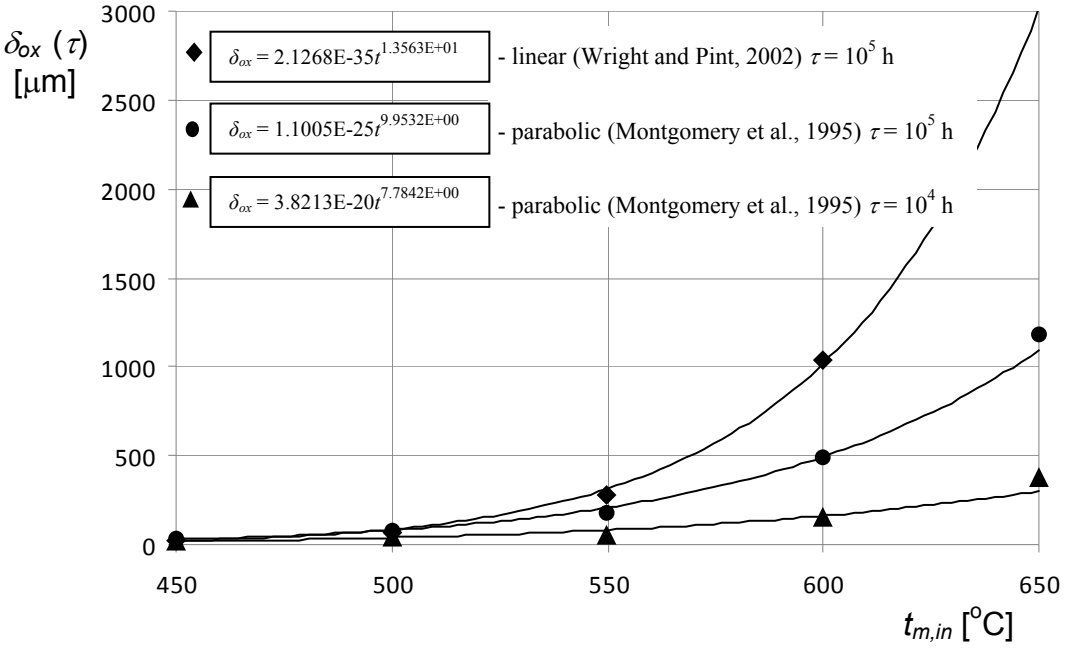

Fig. 4. The rate of oxide scale growth on the inner surface of 10CrMo9-10 tubes versus temperature and time

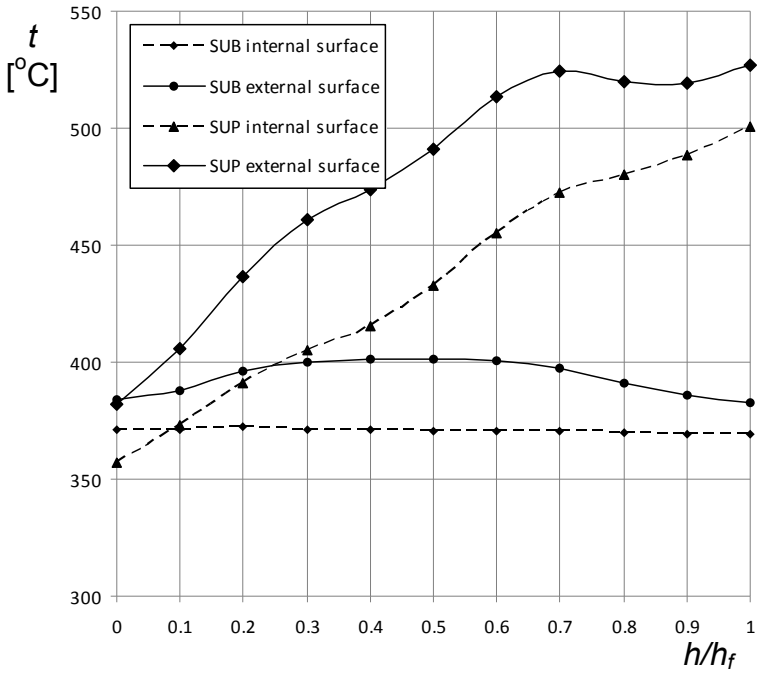

Fig. 5. Temperatures of the middle tube of the waterwall - evaporator with vertical tubes without an internal oxide scale

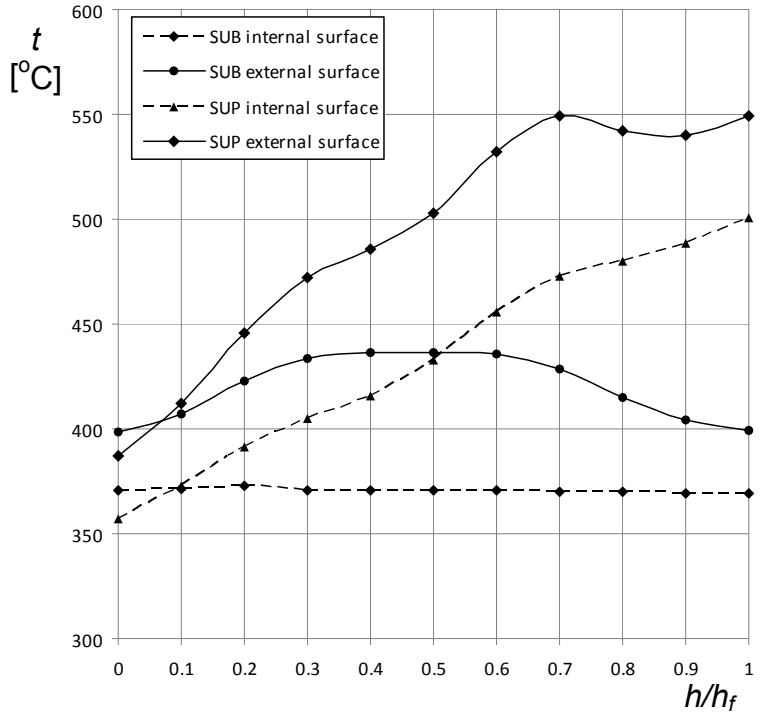

Fig. 6. Temperatures of the middle tube of the waterwall - evaporator with vertical tubes with an internal oxide scale

A varied tube temperature distribution along the tube's height is noticeable in the subcritical and supercritical evaporator. In SUB, because of the essentially constant temperature of the water-steam mixture, changes in the waterwall temperatures reflect the distribution of the transferred heat. In the SUP boiler, the influence of the temperature increase of the water in the tube dominates and therefore at

the end of the waterwall the temperatures in the supercritical boiler are significantly higher than those in the subcritical boiler.

The calculations for the clean tubes and the tubes with an oxide scale show how the temperatures of the waterwall will change in time. The appearance of even a thin oxide layer, which acts as insulation on the inner surface, significantly increases the temperature of the outer surface.

On the basis of the above results, one may draw the following conclusions:

- Waterwalls of supercritical boilers must be made from materials with a much higher durability than those used for subcritical boilers, which will result in a greater temperature increase of the tube because of the lower heat conduction of such types of steel.
- In all processes, the course that intensifies together with an increase in temperature of the wall (slagging, corrosion) will proceed with increased intensity in supercritical boilers.
- The thicker the oxide scale is on the inner wall, the more intensified these processes become.

2.2. Boiler with spiral-wound waterwalls

Systems of spiral-wound waterwalls are made from smooth tubes, where the band that encircles the boiler furnace is narrower than the width of the wall and thus, higher mass fluxes (2000 - 2500 kg/m^{2}s) can be obtained compared with the vertical system. Moreover, if every tube runs through all the walls, the influence of the heat flux variability along the width of the walls, X_{qA_hor}, as shown in Fig. 1, becomes negligible. Thus, one may assume that with a certain simplification, in a boiler with a tangential boiler furnace, the local variability of the heat flux absorbed by every tube of the waterwall at its length is similar to the vertical diversification of the heat flux brought to the waterwalls.

As a result of that, Table 3 shows the conditions that were assumed. The distribution of the transferred heat flux was used for X_{qA_vert} according to Fig. 1. The spiral tubing was characterised by a more balanced distribution of wall temperatures, which is a consequence of the less diversified flux of transferred heat. Moreover, the temperatures of the wall were slightly lower than those occurring in the vertical rifled tubes as a result of increased mass flux of water.

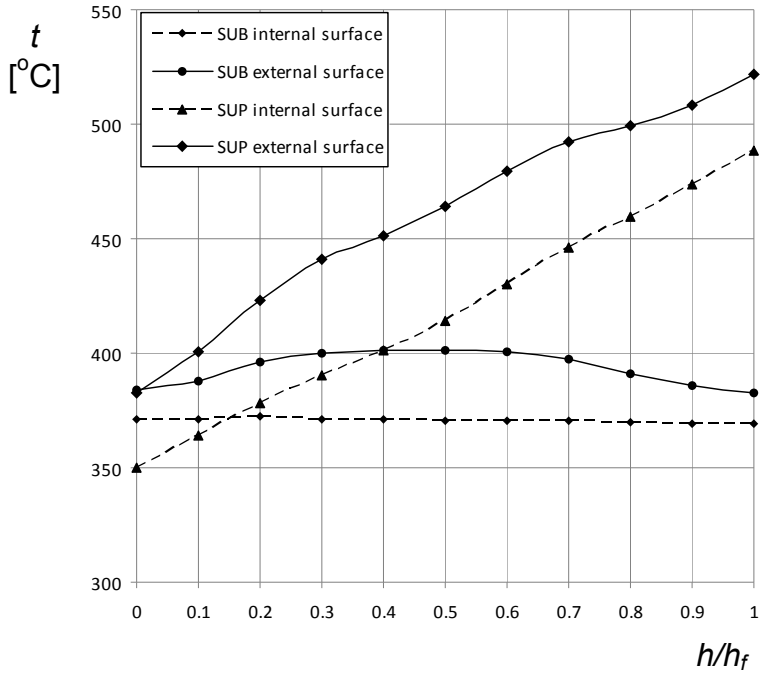

Fig. 7. Temperatures of the waterwall tube - evaporator with spiral-wound tubes without an internal oxide scale

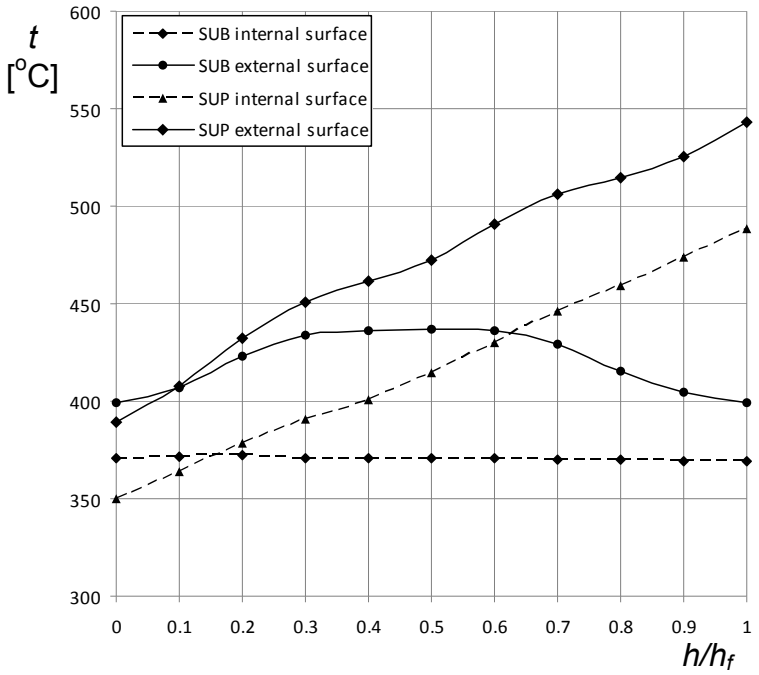

Fig. 8. Temperatures of the waterwall tube - evaporator with spiral-wound tubes with an internal oxide scale

Table 3. Parameters of the supercritical evaporator with a waterwall of spiral tubes

Parameter	Unit	Value
Pressure at inflow	MPa	32.0
Temperature at inflow	°C	340
Pressure at outflow	MPa	31.1
Temperature at outflow	°C	473
Mass flux	kg/m^{2}s	2250
External diameter of tubes	mm	31.8
Internal diameter of tubes	mm	19.8
Mean flux of transferred heat	kW/m^2	159.3
Material	-	HCM2S

At the end of the burner's belt (coordinate 0.5 - Fig. 1), the temperatures of the walls in the spiral system were approximately 30 degrees lower than those in the vertical system, which decreases to some extent and is a hazard of high-temperature corrosion.

3. FUNCTION FOR THE CALCULATION OF THE CORROSION RATE OF THE WATERWALLS IN THE SUPERCRITICAL BOILER

In this study, an attempt was made to assess the corrosion rate of waterwalls with the following assumptions:

- The basic type of corrosion is sulphate and sulphide corrosion, where the intensity depends on CO content in the near-wall flue gas.
- Corrosion is intensified with a temperature increase on the outer surface of the waterwall tubes.

- Chlorine content greater than $Cl \cong 0.1 - 0.2$ % is an additional factor that intensifies corrosion and is commonly recognised as harmless.

Using the above assumptions, the rate of high-temperature corrosion of the waterwalls should be calculated from relationship (Pronobis et al., 2010; Nowak and Pronobis, 2010):

$$w_{corr} = X_{CO}\, w_{corr\,CO}^{max}\, X_{tm}\, X_{Cl} \tag{5}$$

The individual component functions are

$$w_{corr\,CO}^{max} = \frac{\Delta g}{\Delta \tau} = 17.91 CO_{max} + 7.63 \tag{6}$$

$$X_{tm} = 1.82 \cdot 10^{-6}\, t_{m,ex}^{2.224} \tag{7}$$

$$X_{Cl} = 14.64\, Cl^2 - 0.67\, Cl + 1.01 \tag{8}$$

The intensity of corrosion changes during the boiler's operation is primarily a function of changes in CO content in the near-wall flue gas. As Formula (6) refers to conditions in which the rate of tube thickness loss is the highest, a correction is necessary when $X_{CO} \leq 1$, which corrects the $w_{corr\,CO}^{\max}$ to the conditions of the boiler operation in a long period of time during which CO content is occasionally less than CO_{max}:

$$X_{CO} = w_{corr\,CO} / w_{corr\,CO}^{max} \tag{9}$$

where X_{CO} is the correction factor (determined by experiments) that takes into account the lowering of the real corrosion rate of the waterwall tubes in relation to the predicted rate calculated with Formula (6) that assumes $X_{CO} = 1$, i.e., as a result of the lack of maintenance of the maximum CO concentration during the entire tested period.

4. CALCULATION ASSESSMENT OF THE CORROSION HAZARD OF WATERWALLS

On the basis of the formulae described in the previous section, the distribution of the corrosion rate was determined for the middle tube of each wall in the boilers with waterwalls with vertical tubes and for the middle tube with the spiral-wound tubing.

For a real boiler, the basic method to obtain a distribution of CO concentration at different heights consists of taking measurements of the flue gas composition in the near-wall layer. This work is dedicated to a generalised evaluation of differences in the corrosion hazard for boilers with varied structures. Thus, two hypothetical distributions of CO concentration were assumed in the near-wall layer of the flue gas for different heights in the boiler furnace:

- *Distribution 1*: a linear increase from the bottom of the furnace, where the maximum concentration (CO_{max} = 10%) is at 1/4 of the height of the furnace, followed by a linear decrease to the middle of its height;
- *Distribution 2*: constant maximum value (CO_{max} = 5%) to the middle of the furnace height.

At heights above the middle of the furnace, the near-wall layer has, in both distributions, an oxidising character (CO_{max} = 0) due to the corrosion zone in pulverised fuel boilers and is mostly limited to the area of the burner belt and OFA nozzles.

X_{CO} = 1 and Cl = 0.05% were assumed for the calculations. For both distributions, the same content of Cl in the fuel was assumed. The variability of the corrosion hazard of the tubes results only from the

differences in the distribution of the temperatures of the waterwall tubes and the nature of the changes in the content of CO in the boundary layer of the flue gas.

The local values of the corrosion rate along the chosen tubes were calculated using Equation (5). The received results are presented in Figs. 9 and 10.

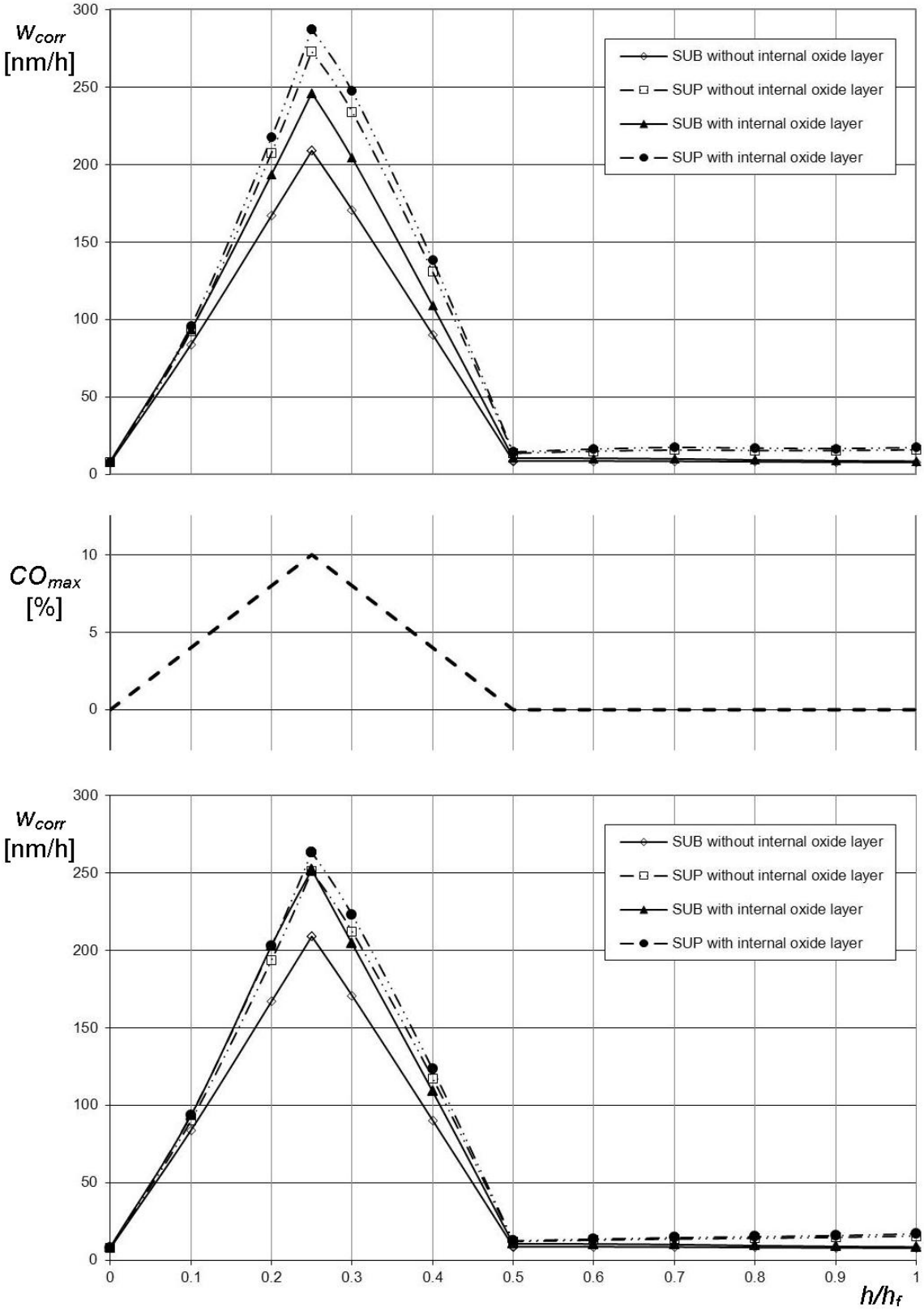

Fig. 9. Rate of corrosion loss of vertical tubes (top graph) and spiral tubes (bottom graph) for *Distribution 1* of CO in the near-wall layer of the flue gas

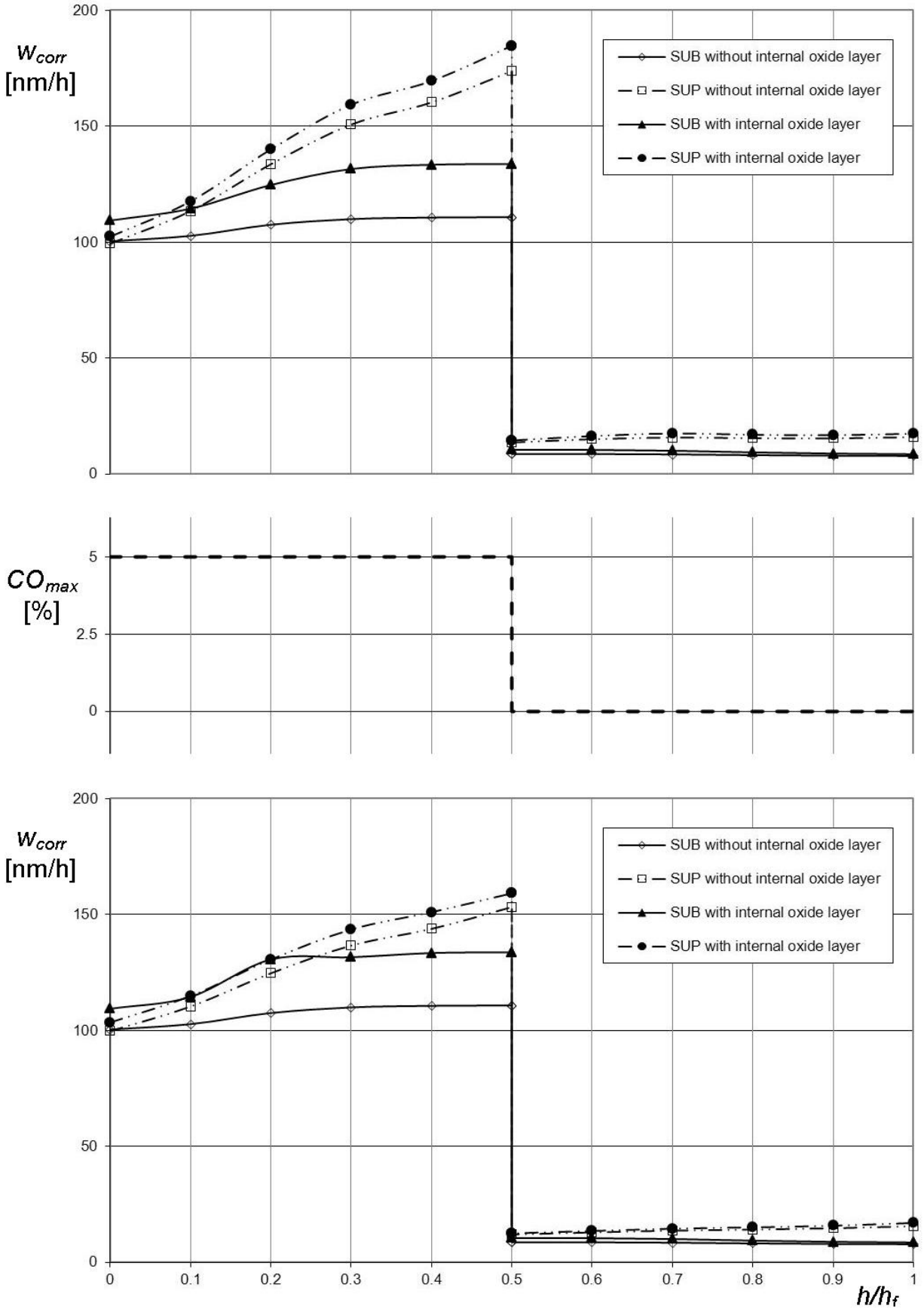

Fig. 10. Rate of corrosion loss of vertical tubes (top graph) and spiral tube (bottom graph) for *Distribution 2* of CO in the near-wall layer of the flue gas

At the variable content of CO in the near-wall layer, the corrosion rate reached the highest value at the point when CO_{max} = 10%, whereas at a constant content of CO in the near-wall layer (CO_{max} = 5% from the bottom to the middle of the furnace height), the corrosion rate reached its maximum at the point at the maximum temperature of the outer tube wall, i.e., where there was an abrupt change of CO content in the flue gas.

The variability of the corrosion rate along the height of the boiler furnace depended on a temperature increase on the outer wall of the waterwall tube. For subcritical boilers with a waterwall of tubes without an internal oxide layer, the tube thickness loss depended almost exclusively on the changes in CO content in the near-wall layer of the flue gas because the increase in the tube temperature was relatively small and thus, the function differs slightly from the constant in both scopes for the determined value of CO content. A monotonically increasing temperature of the outer wall of the waterwall tube of the supercritical boilers also translates into a quasi-linear course of the distribution of the corrosion rate in those particular areas of the waterwalls. Only the distribution of the corrosion loss for the subcritical evaporator with a waterwall of tubes with an internal scale stands out with its curved graph corresponding to the heat flux transferred to the waterwall tubes.

The difference between the distribution of the corrosion rate for the waterwalls with the vertical tubes and that with the spiral ones results from differences in the distribution of the wall temperatures of the heated surfaces, as shown in Figs. 5-8. Analogically, the distribution of the rate of corrosion is also affected by the presence of an internal oxide scale in the waterwall tubes or its absence.

At the top of the boiler furnace, where a zero value of CO was assumed in the near-wall layer of the flue gas, the rate of corrosion reached values corresponding to the typical rate of steel oxidation during contact with flue gas containing oxygen, and its distribution depended exclusively on the external temperature of the tube wall. Thus, the rate of corrosion from the middle of the boiler furnace to its top will slightly decrease in the subcritical boilers and slightly increase in supercritical boilers.

For a quantitative assessment of differences between the hazard of the low-NOx corrosion in the subcritical boilers and in the supercritical boilers, one may also use Formula (7). If we assume that in the compared boilers, the same fuel is combusted in the same conditions, then the values of w_{corrCO}, X_{Cl} and X_{CO} in Eq. (5) should be the same for the sub- (SUB) and supercritical (SUP) boilers. Then, the relation for the corrosion rate in the compared boilers can be given by:

$$w_{corr\,SUP/SUB} = \frac{X_{tm\,SUP}}{X_{tm\,SUB}} = \left(\frac{t_{m,ex\,SUP}}{t_{m,ex\,SUB}} \right)^{2.224} \tag{10}$$

The effect of the waterwall tube working conditions on the corrosion rate is given by the results of the calculations presented in Table 4, which compares w_{corr} at a level of h/h_f = 0.5, (Fig. 1). The following cases were compared with the temperature values from Figs. 5-8:

- *Variant A*: ratio of the corrosion rate in the supercritical boiler with vertical tubes and the subcritical boiler without internal fouling,
- *Variant B*: ratio of the corrosion rate in the supercritical boiler with vertical tubes and the subcritical boiler with internal fouling (after 10^5 h of operation),
- *Variant C*: ratio of the corrosion rate in the supercritical boiler with spiral tubing and the subcritical boiler without internal fouling,
- *Variant D*: ratio of the corrosion rate in the supercritical boiler with spiral tubing and the subcritical boiler with internal fouling (after 10^5 h of operation).

Table 4 shows that a supercritical boiler needs to deal with a significantly (20 to 60 %) higher rate of corrosion of waterwalls compared with in a subcritical boiler. The hazard is intensified at the top of the burner belt as a result of a constant increase of the water temperature in the supercritical tubes. The

temperatures of the walls in the spiral system are approximately 30 degrees lower than those in the vertical system which, to some extent, decreases the hazard of high-temperature corrosion. The increase in the corrosion rate in the supercritical evaporator after a longer operation period was slightly smaller, which is only the result of a faster formation of the internal oxide scale in the subcritical evaporator for comparable cases. It should also be noted that under normal conditions, a smaller corrosion rate there is likely to occur in the supercritical waterwalls because of the sliding pressure operation when the boiler is partly operated in the subcritical mode.

Table 4. Comparison of the corrosion rate in the sub- and supercritical boilers

Variant	$t_{m,ex\ SUP}$ [°C]	$t_{m,ex\ SUB}$ [°C]	$w_{corr\ SUP/SUB}$
A	491.3	401.2	1.569
B	504.9	436.7	1.381
C	464.2	401.2	1.383
D	472.2	436.7	1.190

5. CONCLUSIONS

The results show that the variability of the corrosion rate along the height of the boiler furnace depends on the temperature increase of the external tube surface and on the distribution of the local CO concentration. The oxide scale on the inner surface of the tubes is an additional factor that significantly increases the corrosion hazard. The calculations showed that the supercritical boilers exhibited a significantly higher rate of corrosion in the waterwalls than the subcritical boilers. Because the temperature of the walls in the spiral system was lower than that in the rifled vertical system, the high-temperature corrosion hazard was also slightly smaller with such a tubing structure.

At the top of the boiler furnace, where a zero value of CO was assumed in the near-wall layer of the flue gas, the rate of corrosion reached values corresponding to the typical rate of steel oxidation when in contact with flue gas containing oxygen, and its distribution depended exclusively on the external temperature of the tube wall. Thus, the rate of corrosion from the middle to the top of the boiler furnace will slightly decrease in subcritical boilers and slightly increase in supercritical boilers.

SYMBOLS

Cl	chlorine content in the fuel; as received basis, -
CO_{max}	maximum content of CO in the tested period in the boundary layer of the flue gases; dry basis, %
c_p	specific heat of water, kJ/(kgK)
$\overline{c}_p$	mean specific heat of water, kJ/(kgK)
d	internal diameter of tube, m
h	specific enthalpy of water, kJ/kg
h/h_f	relative furnace height, -
L	length of tube, m
Nu	Nusselt number, -
p	pressure, Pa
Pr	Prandtl number, -
q_A	cross-sectional heat load of the waterwall, kW/m^2

q_V	volumetric heat load of the furnace, kW/m^3
Re	Reynolds number, -
t	temperature, °C
w	flow velocity of water in the tube, m/s
w_{corr}	rate of high-temperature corrosion of the waterwalls, nm/h
w_{corrCO}	rate of high-temperature corrosion of the waterwalls caused by CO, nm/h
w/w_f	relative furnace width, -
X_{Cl}	chlorine content correction factor, -
X_{CO}	CO content correction factor, -
X_{qA}	local heat load related to the mean heat load of the waterwall, -
X_t	temperature correction factor, -

Greek symbols

α	heat transfer coefficient between the subcritical steam and the water mix, W/(m^{2}K)
$\Delta g/\Delta\tau$	maximum rate of local tube thickness loss along its perimeter, nm/h
δ_{ox}	thickness of the oxide layer, μm
λ	thermal conductivity of water, W/(mK)
μ	dynamic viscosity of water, Pas
ρ	density of water, kg/m^3
τ	time, h

Subscripts

m,ex	waterwall tube material, external surface
m,in	waterwall tube material, internal surface
max	maximum
wm	mean value for water parameters
hor	horizontal
SUB	subcritical
SUP	supercritical
vert	vertical

REFERENCES

Bukowski P., Hardy T., Kordylewski W., 2009. Evaluation of corrosion hazard in PF boilers applying the oxygen content in flue gases. *Archiwum Combustionis*, 29, 11-18.

Franke J., Kral R., 2003. Supercritical boiler technology for future market conditions. *Parsons Conference*, October 2003, 1-13.

Grabezhnaja W.A., Kirillow P.L., 2006. Heat transfer under supercritical pressures and heat transfer deterioration boundaries. *Therm. Eng.*, 53, 296-301. DOI: 10.1134/S0040601506040069.

Harb J.N., Smith E.E., 1990. Fireside corrosion in PC-fired boilers. *Prog. Energy Combust. Sci*., 16., 169–190. DOI: 10.1016/0360-1285(90)90048-8.

Karcz H., Miller R., Jodkowski W., Ładogórski P., 2005. Sulfur content and its forms in Polish boiler coals. *Chem. Process Eng.*, 26, 27-33.

Montgomery M., Karlsson A., 1995. Oxidation of new types of steel in steam-side conditions. *VGB Kraftwerkstechnik*, 75, H. 3., 258-264 (in German).

Nowak W., Pronobis M. (Eds.), 2010. *Advanced technologies for combustion and flue gas treatment*. *Wydawnictwo Politechniki Śląskiej*, Gliwice (in Polish).

Orłowski P., Dobrzański W., Szwarc E., 1979. *Steam boilers*. WNT, Warszawa (in Polish).

Palkes M., Sadlon E. S., Salem A., 1994. State-of-the-art large capacity sliding pressure supercritical steam generators. *AEB - SPERI Power Generation Conference 1994*.

Pronobis M., Hernik B., Wejkowski R., 2010. Kinetics of low NOx corrosion of waterwalls in utility boilers. *Rynek Energii*, 6 (91), 121- 128.

Rassohin N. G., Shvecov R. S., Kuzmin A. W., 1970. Calculation boiling heat transfer. *Teploenergetika*, 9, 58 (in Russian).

Rusin A., Wojaczek A., 2009. Influence of thermal loads variation on the probability of waterwall tubes corrosion failure in low-emission combustion. *Rynek Energii*, 6(85), 129-133 (in Polish).

Wagner W., Cooper J.R., Dittmann A., Kijima J., Kretzschmar H.-J., Kruse A., Mares R., Oguchi K., Sato H., Stöcker I., Sifner O., Takaishi Y., Tanishita I., Trübenbach J., Willkommen Th., 2000. The IAPWS Industrial Formulation 1997 for the thermodynamic properties of water and steam, *ASME J. Eng. Gas Turbines Power*, 122, 150-185. DOI:10.1115/1.483186.

Wright I. G., Pint B. A., 2002. An assessment of the high-temperature oxidation behavior of Fe-Cr steels in water vapor and steam. *NACE Corrosion/2002*, Denver, April 8-11, 2002. Paper No. 02377.

Received 21 September 2011
Received in revised form 09 June 2012
Accepted 14 June 2012